Noncontact Ultrasonic Sensing for Seam Tracking in Arc Welding Processes

S. B. Zhang

Y. M. Zhang
Mem. ASME

Welding R&D Laboratory,
Center for Robotics and
Manufacturing Systems,
University of Kentucky,
Lexington, KY 40506

R. Kovacevic
Southern Methodist University,
Dallas, TX

A novel seam tracking technology based on high frequency ultrasound is developed in order to achieve high accuracy in weld seam identification. The transmission efficiency of the ultrasound is critical for obtaining a sufficient echo amplitude. Since the transmission efficiency is determined by the difference in impedance between the piezoelectric ceramic and air, match layers are designed to optimize the transmission efficiency by matching impedance. Since the air impedance depends on the density and velocity of the ultrasound, which both depend on the temperature, the optimization has been done for a wide bandwidth. Also, the receiving circuit is designed so that its resonance frequency matches the frequency of the ultrasound. As a result, the sensitivity of the noncontact ultrasonic sensor is improved 80-fold. By properly designing the focal length of the transducer, a high resolution ultrasound beam, 0.5 mm in diameter, is achieved. Based on the proposed sensing technology, a noncontact seam tracking system has been developed. Applications of the developed system in gas tungsten arc welding (GTAW) and CO_2 gas metal arc welding (GMAW) processes show that a tracking accuracy of 0.5 mm is guaranteed despite the arc light, spatter, high temperature, joint configuration, small gap, etc.

1 Introduction

Seam tracking plays a fundamental and critical role in generating sound arc welds [1–3]. A number of seam tracking approaches have been proposed. Through-the-arc sensing is based on the correlation between the arc length and arc voltage. Because of its robustness against smoke, spatter, and arc radiation, it is the most prevalent method for seam tracking today [4]. However, in order to apply this technique, the joint sidewalls must be well defined or have a groove. Also, the mandatory weave of the torch causes an undesired coupling between the sensing and the welding process. In optical sensing, either a laser stripe or a scanned laser spot is projected onto the weld seam region. In this method, the seam and joint geometry [4–6] can be accurately determined based on the triangulation principle. Also, this method can measure the geometry of the sag [7] which contains useful seam information for multiple pass welding. However, the system is relatively expensive and its performance is influenced by smoke, spatter, and arc radiation. In order to minimize such influence, the joint is usually previewed ahead of the arc.

Among the proposed approaches is the noncontact ultrasonic sensing which will be improved in this work. The principle behind this method is that the propagation interval for the ultrasound in air is related to the distance between the ultrasound source and the reflection point and the distance between the reflection point and the receiver. The noncontact ultrasonic sensor was first introduced to seam tracking in the early 1980's by Estochen [1]. Umeagukwu [2] used a 100 kHz airborne ultrasonic transducer to measure the joint orientation and lateral deviation caused by curvature or discontinuities in the part. A data acquisition system was developed for V-groove joints and lap joints. Recently, Beodiano [8] used a 220 kHz piezoelectric transducer to detect the geometry of the seam through periodic sampling of the echo amplitude. Experimental results demonstrated that ultrasonic sensors can be used for seam tracking in arc welding processes.

Contributed by the Manufacturing Engineering Division for publication in the JOURNAL OF MANUFACTURING SCIENCE AND ENGINEERING. Manuscript received Jan. 1997; revised July 1997. Associate Technical Editor: S. G. Kapoor.

Although the noncontact ultrasonic sensors have shown significant advantages such as low cost, simple configuration, and

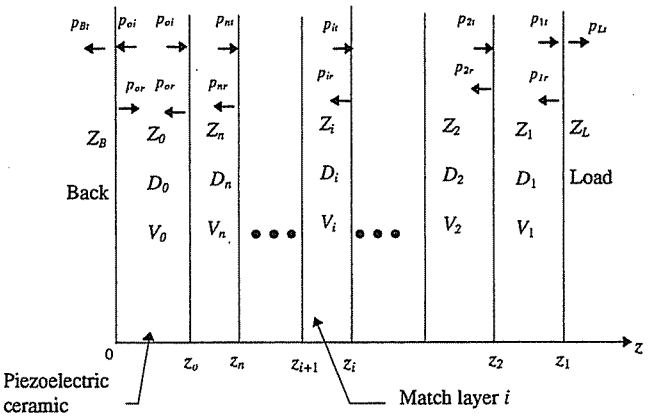

Fig. 1 Configuration of ultrasonic sensor with load matching layers

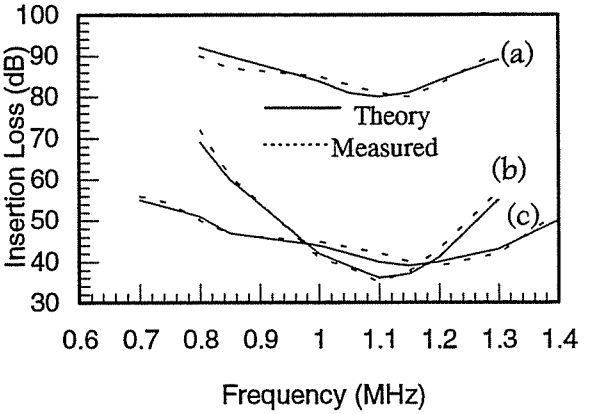

Fig. 2 Two-way insertion loss (*a*) without match (*b*) single match layer (*c*) two match layers

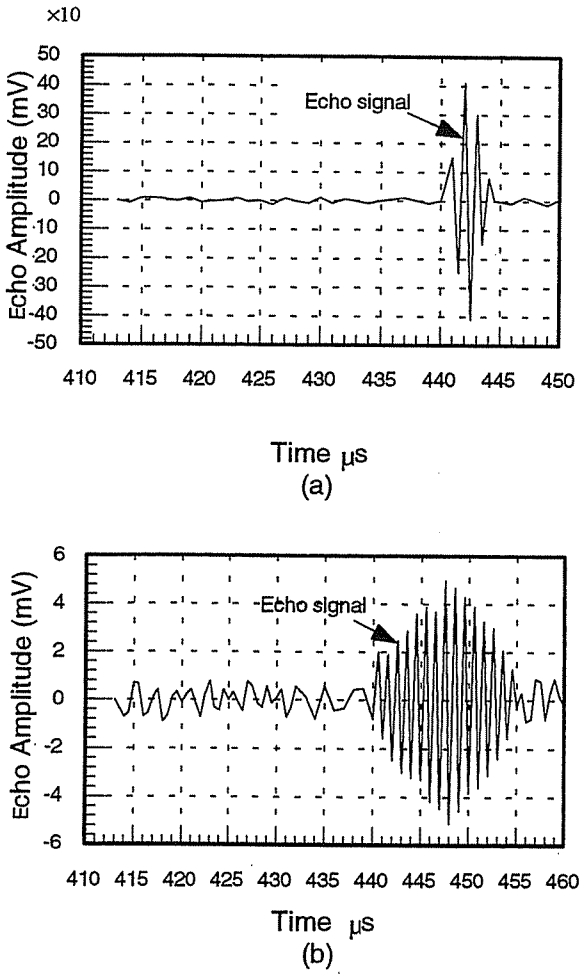

Fig. 3 Experimental measurements of pulse responses (*a*) with double match layer (*b*) without match layer

robustness against the arc-light, spatter, and dust, the sensors have been the conventional electrostatic air ultrasonic sensors [9] or bending mode piezoelectric air ultrasonic sensors [10] operating below 100 kHZ [11, 12]. In general, the width and wavelength of the ultrasound beam increase as the frequency decreases. Lower frequencies therefore correspond to poorer resolutions, but longer travel distances. For traditional applications of noncontact ultrasonic sensors, i.e., long distance measurement of large targets, such sensors are suitable. However, it is very difficult for such sensors to identify a seam in butt welding because of the small gap and relatively short distance. In addition, noise in an arc welding environment is mainly concentrated in a frequency range below 1000 kHz [1]. To overcome the noise and obtain better beam resolutions, high-frequency ultrasounds should be used.

In this work, high-frequency ultrasound based seam tracking is addressed. Unlike low-frequency ultrasound, high-frequency ultrasound significantly decays in air. In order to achieve a sufficient amplitude of the echo despite the high frequency, the transmission efficiency of the ultrasound from the piezoelectric ceramic to the air is maximized based on impedance match. It is known that impedance of the air is dependent on the temperature. During arc welding, the temperature and temperature gradient are high. Thus, the impedance of the air varies. The impedance match must be robust to the variation in the temperature. To increase the system sensitivity, the impedance match is also done in the receiving circuit. In addition, a focused transducer is designed to improve the lateral resolution. Experiments show that the developed system can accurately track the seam in different arc welding processes.

2 Acoustic Impedance Match

Thickness-driven mode ultrasounds are associated with directional propagation and good focusing ability. Such properties are critical in achieving better resolution. Hence, thickness-driven mode ultrasonic transducers are used in this work.

The main problem with the thickness-driven high frequency transducer in seam tracking applications is the large mismatch between the piezoelectric ceramic and load (air). The large mismatch causes the majority of the acoustical energy to be reflected back and forth between the rear and front face of the ceramic. The acoustic transmission coefficient on the transducer-load interface is very low if no match layer is added. A proper use of match layers between the transducer and load can increase the sensitivity, bandwidth and impulse response of the transducer by improving on the transmission efficiency.

The propagation of sound waves emitted by a thickness-driven mode piezoelectric ceramic with match layers in a low impedance load may be described as (Fig. 1) [13]:

$$\begin{cases} p_{oi}(z,\tau) = P_{oi}e^{j[\omega\tau - k_o z]} & (0 \le z \le z_o) \\ p_{or}(z,\tau) = P_{or}e^{j[\omega\tau + k_o z]} & (0 \le z \le z_o) \\ p_{it}(z,\tau) = P_{it}e^{j[\omega\tau - k_i(z - z_{i+1})]} & (1 \le i \le n;\ z_{i+1} \le z \le z_i) \\ p_{ir}(z,\tau) = P_{ir}e^{j[\omega\tau + k_i(z - z_{i+1})]} & (1 \le i \le n;\ z_{i+1} \le z \le z_i) \\ p_{Lt}(z,\tau) = P_{Lt}e^{j[\omega\tau - k_L(z - z_1)]} & (z_1 \le z) \\ p_{Bt}(z,\tau) = P_{Bt}e^{j[\omega\tau + k_B z]} & (z \le 0) \end{cases} \tag{1}$$

where z is the coordinate along the thickness direction, τ is the time, p is the acoustic pressure, P is the oscillating amplitude of acoustic pressure, $\omega = 2\pi f$, f is the frequency of the ultrasound, and k denotes the propagation number in a respective material [13]. The subscripts o, i $(1 \le i \le n)$, L, and B represent the ceramic, the i^{th} match layer, the load, and the

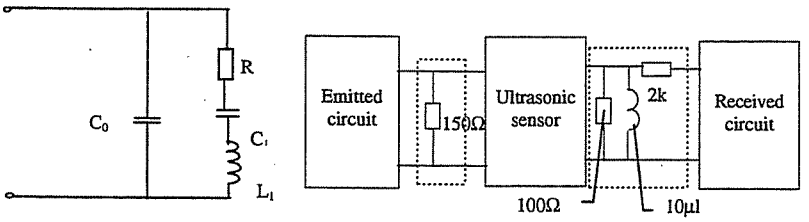

a. Equivalent circuit of ultrasonic sensor.

b. A circuit

Fig. 4 Equivalent circuit of transducer and matching circuit

Table 1 Measured parameters of 1.15 MHz noncontact ultrasonic sensor

F_o	Q	C_o	C_1	L_1	R_1
1153kHz	6.1	2.2 nF	1.07E-01 nF	0.74 mH	182.5ohm

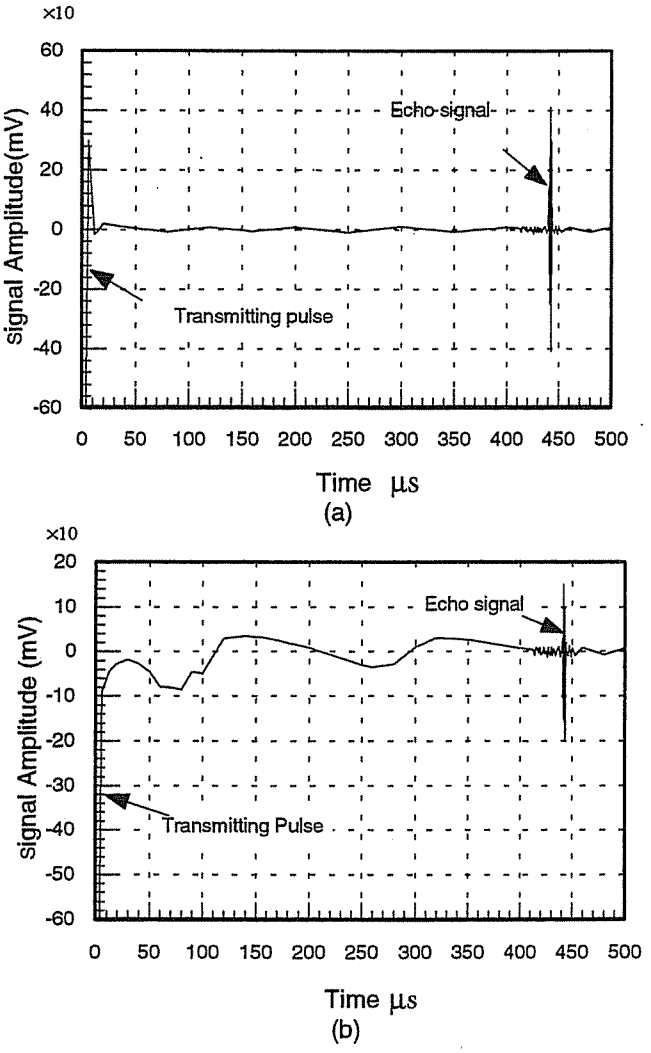

Fig. 5 Experimental measurements of pulse responses (*a*) with circuit match (*b*) without circuit match

back, and the subscripts r and t denote the reflected and transmitted wave of the ultrasound. The subscript e denotes the wave emitted by the transducer. In Fig. 1, Z's, V's, and D's denote the acoustic impedance, speed, and thickness corresponding to their subscripts. The open-circuit resonant frequency is denoted by f_0.

The reflection coefficient R and transmission coefficient T in each interface can be obtained based on the continuity of the sound pressure and the vertical oscillation speed on the interface [13]:

$$
\begin{cases}
R_{on} = |p_{or}(z,\tau)/p_{oi}(z,\tau)|_{z=z_o} = \dfrac{Z_n - Z_o}{Z_n + Z_o} \\
T_{on} = |p_{nt}(z,\tau)/p_{oi}(z,\tau)|_{z=z_o} = \dfrac{2Z_n}{Z_n + Z_o} \\
R_{i(i-1)} = |p_{ir}(z,\tau)/p_{it}(z,\tau)|_{z=z_i} = \dfrac{Z_{i-1} - Z_i}{Z_{i-1} + Z_i} \quad (2 \le i \le n) \\
T_{i(i-1)} = |p_{(i-1)t}(z,\tau)/p_{it}(z,\tau)|_{z=z_i} = \dfrac{2Z_{i-1}}{Z_{i-1} + Z_i} \quad (2 \le i \le n) \\
R_{L1} = |p_{Lr}(z,\tau)/p_{1t}(z,\tau)|_{z=z_1} = \dfrac{Z_L - Z_1}{Z_L + Z_1} \\
T_{L1} = |p_{Lt}(z,\tau)/p_{1t}(z,\tau)|_{z=z_1} = \dfrac{2Z_L}{Z_L + Z_1} \\
R_{Bo} = |p_{Br}(z,\tau)/p_{oi}(z,\tau)|_{z=0} = \dfrac{Z_B - Z_o}{Z_B + Z_o} \\
T_{on} = |p_{nt}(z,\tau)/p_{ot}(z,\tau)|_{z=0} = \dfrac{2Z_B}{Z_B + Z_o}
\end{cases}
\tag{2}
$$

Equations (2) show that a large difference of the acoustic impedance between two different media corresponds to a low transmission efficiency, but a high reflection coefficient. It is known that the acoustic impedance of the piezoelectric ceramic is about 10^7 kg/m^{2}s [14]. However, the acoustic impedance of the air is only 4×10^2 kg/m^{2}s [14]. If no match layer is used, most of the acoustic energy generated by the transducer will be reflected back and forth between the rear and front face of the ceramic so that only a very tiny portion of the acoustic energy will be transmitted to the air. Match layers must be used and properly designed.

According to Mason's equivalent circuit [15], a thickness-driven mode ultrasonic transducer with match layers can be described using the model shown in Fig. 1. If the transverse dimensions of the match layers are much larger than their thicknesses, the input impedance of a transmission line which

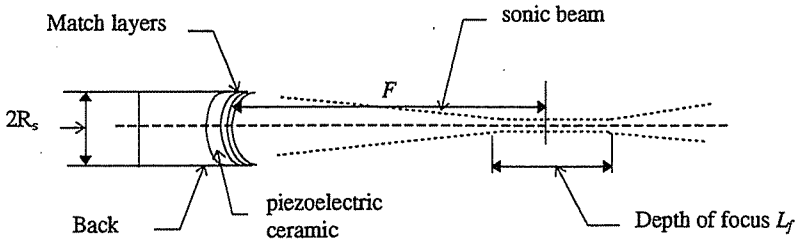

Fig. 6 Configuration of ultrasonic transducer with match layers

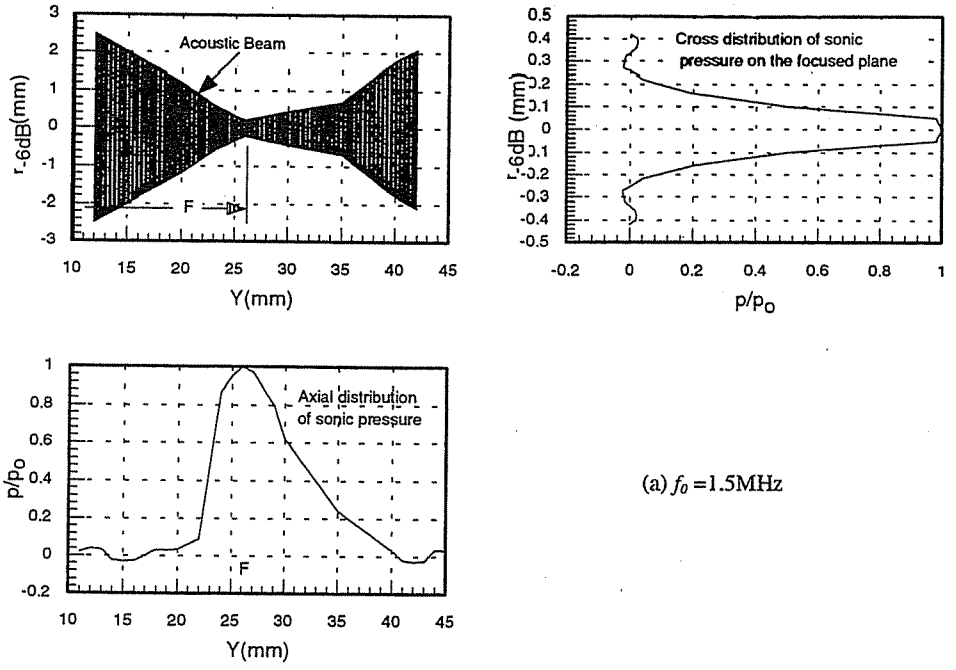

(a) f_0 =1.5MHz

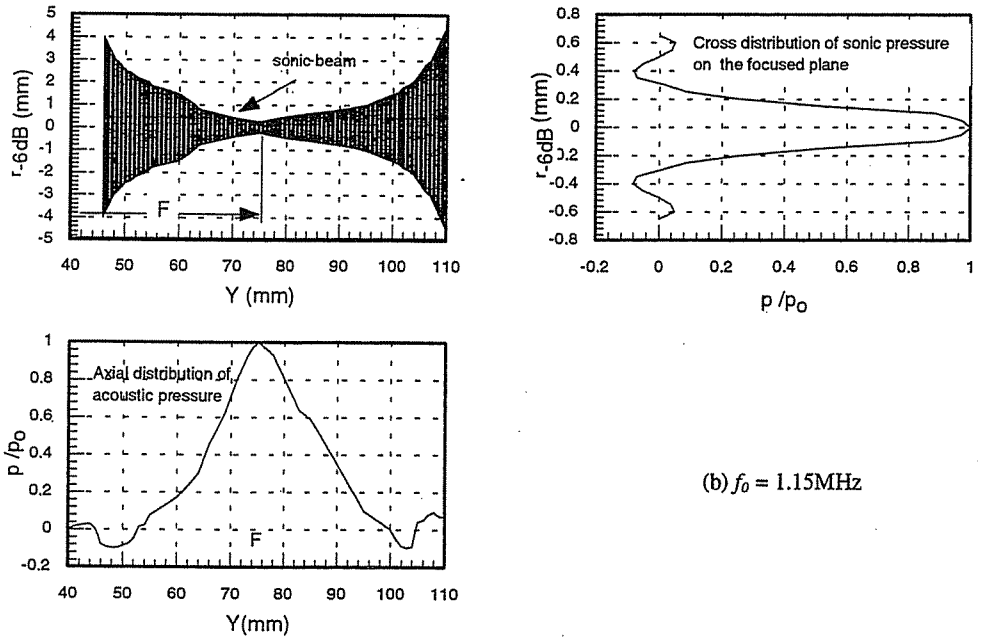

(b) f_0 = 1.15MHz

Fig. 7 Experimental measurements of acoustic pressure distribution of the focused ultrasonic sensor (*a*) f_0 = 1.5 MHz (*b*) f_0 = 1.15 MHz (*c*) f_0 = 0.4 MHz

starts at layer i and terminates by the load can be calculated using the following recursive Eq. [16]:

$$\begin{cases} Z_{L,i}(f) = \dfrac{Z_i(Z_{L,i-1}\operatorname{Cos}\theta_i + jZ_i\operatorname{Sin}\theta_i)}{Z_i\operatorname{Cos}\theta_i + jZ_{L,i-1}\operatorname{Sin}\theta_i} & (2 \le i \le n) \\ Z_{L,1}(f) = \dfrac{Z_1(Z_L\operatorname{Cos}\theta_1 + jZ_1\operatorname{Sin}\theta_1)}{Z_1\operatorname{Cos}\theta_1 + jZ_L\operatorname{Sin}\theta_1} \end{cases} \quad (3)$$

where $\theta_i = 2\pi D_i/\lambda_i(f)$ $(1 \le i \le n)$, and $\lambda_i(f)$ is the wavelength of the ultrasound in layer i at the frequency f. For the convenience of discussion, we refer to the net acoustic load of the transducer as the generalized load of the transducer and denote its impedance as $Z_{L'}$. For a transducer that has n match layers, $Z_{L'} = Z_{L,n}$.

Consider the case with a single match layer. At so-called quarter wave frequencies $f_t's$ defined by

$$D_1 = (2m + 1)\lambda_1(f_t)/4 \quad (4)$$

for integer m, $Z_{L'}(f_t) = Z_{L,1}(f_t)$ is real [16]:

$$Z_{L,1}(f_t) = Z_1^2/Z_L \quad (5)$$

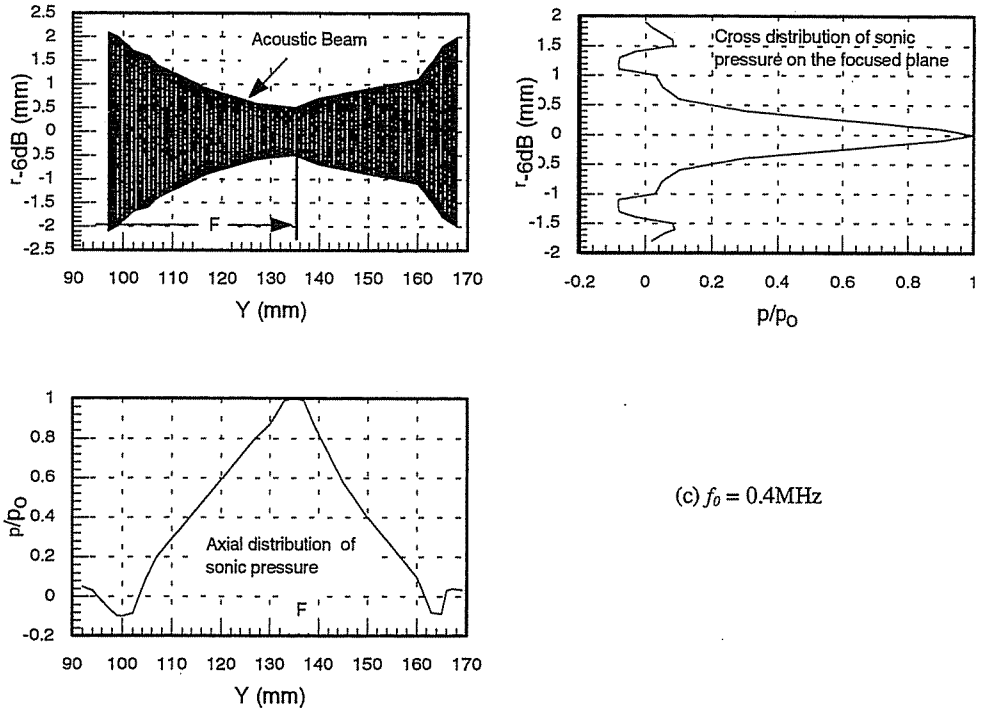

(c) $f_0 = 0.4$MHz

Fig. 7 (Continued)

Thus, $Z_{L'}(f_t)$ can be controlled by selecting the impedance of the match layer (Z_1). A good acoustic impedance match to the transducer at f_t can be obtained by selecting:

$$Z_1 = \sqrt{Z_o Z_L}\,. \tag{6}$$

At frequency $f \neq f_t$, $Z_{L'}(f)$ is complex. However, when Z_1 is selected based on (6), $Z_{L'}(f)$ remains close to Z_o in a substantial neighborhood of f_t and a good impedance match is brought about over a broad bandwidth.

In order to achieve a good match, two quarter-wave match layers are used in this work. In this case,

$$Z_{L'}(f_t) = Z_{L,2}(f_t) = Z_L Z_2^2/Z_1^2 \tag{7}$$

It is apparent that $Z_{L'}(f_t)$ can be controlled by Z_2/Z_1. Thus, an acoustic impedance match can be achieved by selecting Z_2/Z_1 so that $Z_{L'}(f_t) \approx Z_o$:

$$Z_L Z_2^2/Z_1^2 \approx Z_o \tag{8}$$

For determining the actual values of Z_1 and Z_2, one can choose the impedance of the match layers so that the impedance from the transducer, layer 2, layer 1, to the load decays approximately at the same ratio. That is,

$$Z_o/Z_2 \approx Z_1/Z_L \tag{9}$$

Hence, from (8) and (9), the following match equations can be obtained:

$$\begin{cases} Z_1 \approx \sqrt[4]{Z_o Z_L^3} \\ Z_2 \approx \sqrt[4]{Z_o^3 Z_L} \end{cases} \tag{10}$$

The match Eqs. (6) and (10) are obtained at the quarter-wave frequencies $f_t(m)$'s ($m = 0, 1, 2, \ldots$) defined in (4). In this work, the resonance frequency of the transducer, f_0, is selected as f_t ($m = 0$), i.e., the quarter-wave frequency for $m = 0$. Thus, the match Eqs. (6) and (10) can be used to design the match layers.

The material of the piezoelectric ceramic is PZT-5A. Its acoustic impedance $Z_o = 3.45 \times 10^7$ kg/m^{2}s. The impedance of the load (air) is $Z_L = 4 \times 10^2$ kg/m^{2}s. Based on Eq. (10), $Z_2 = 2 \times 10^6$ kg/m^{2}s and $Z_1 = 7 \times 10^3$ kg/m^{2}s. However, no material has an acoustic impedance close to Z_1. Based on the approximation of the optimal impedance and the acoustic attenuation of the match material, the acoustic impedance of the selected material for match layer 1 is 1.5×10^5 kg/m^{2}s. The impedance of the material for match layer 2 is 2×10^6 kg/m^{2}s. The materials for both layer 1 and layer 2 are composites of silicone rubber. In the case of a single layer, the impedance of the match layer is 2×10^5 kg/m^{2}s. Its material is also a composite of silicone rubber.

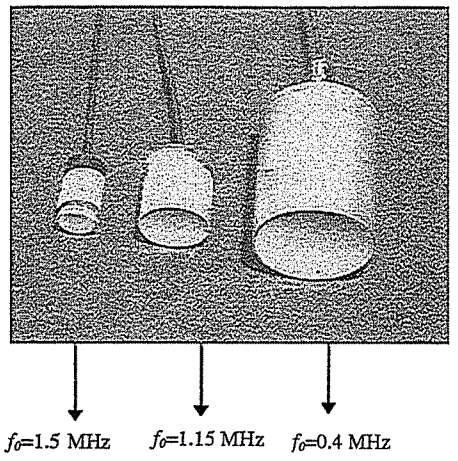

Fig. 8 Noncontact ultrasonic sensors

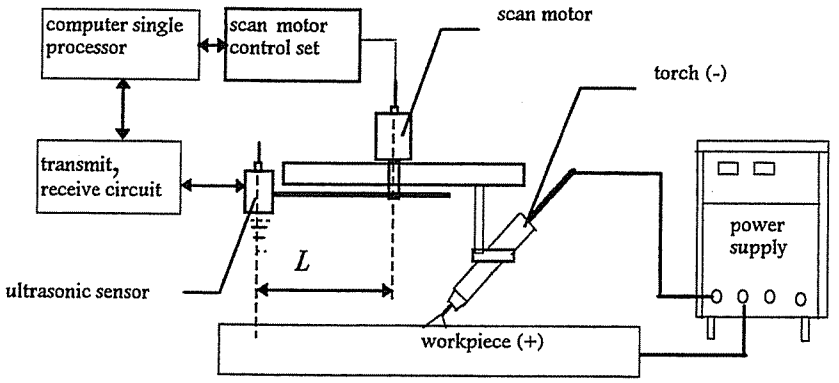

Fig. 9 Noncontact ultrasonic tracking system

In order to examine the performance of the designed acoustic match, transmission experiments have been done. Figure 2 shows the calculated and experimentally measured loss for different transducers: without match layer, with a single match layer, and with double match layers. The resonance frequency of the transducer, which is determined by the material and thickness of the piezoelectric ceramic, with a backing load of 5×10^6 kg/m^{2}s is $f_0 = 1.15$ MHz. The calculations are performed based on Mason's equivalent circuit. Figure 2 shows that the theoretical calculations are very close to the experimental measurements. It can be observed that the utilization of the match layers greatly improves the transmission efficiency despite the approximation of the actually used impedance of match layer 1. Compared with a single match layer, double layers significantly increase the bandwidth of the acoustic match. For the application of arc welding where the high temperature and high temperature gradient are substantial, double match layers provide a robust acoustic impedance match.

Figure 3(a) plots the measured two-way insertion response of the designed transducer to a pulse signal. In this case, the amplitude of the pulse response reaches ±400 mV and its duration lasts only 3 μs. However, if no match layers are used, the amplitude of the pulse response is only ±5 mV, and the duration is 12 μs [Fig. 3(b)]. Thus, the acoustic impedance match significantly improves the transmission efficiency of the ultrasound so that a noncontact high frequency ultrasound can be used to increase the resolution.

3 Circuit Impedance Match

To further improve the sensitivity of the noncontact ultrasonic sensor, its circuit impedance match is also necessary. The impedance property of a piezoelectrically excited vibrator can be approximately represented by an isolated lumped-parameter resonance equivalent circuit [17] (Fig. 4(a)). In Fig. 4(a),

$$C_0 = \epsilon_{33}^s A / D_o \tag{11}$$

$$C_1 = \tfrac{1}{2}\pi f_0 R_1 Q \tag{12}$$

$$L_1 = \tfrac{1}{2}\pi f_0 C_1 \tag{13}$$

where

A: effective area of the transducer,
ϵ_{33}^s: capacity coefficient of the sensor,
C_0: parallel capacitance of the vibrator,
C_1: motional capacitance of the vibrator,
L_1: motional inductance of the vibrator,
R_1: motional resistance which in the equivalent circuit represents the mechanical dissipation of the piezoelectric resonator, and
Q: quality factor of the piezoelectric resonator.

The parallel capacitor C_0 of the sensor will influence the resonance frequency of L_1 and C_1. Circuit impedance match will reduce C_0's effect on the resonance frequency of the sensor

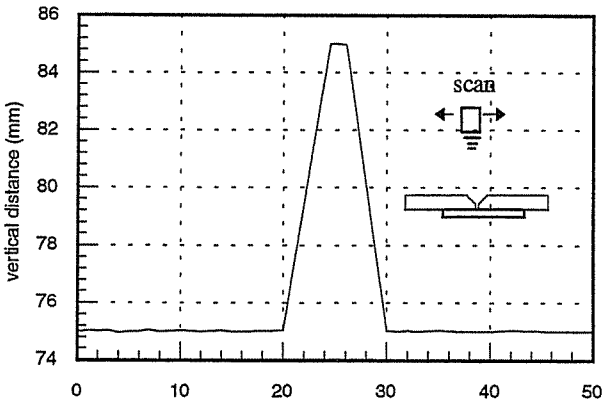

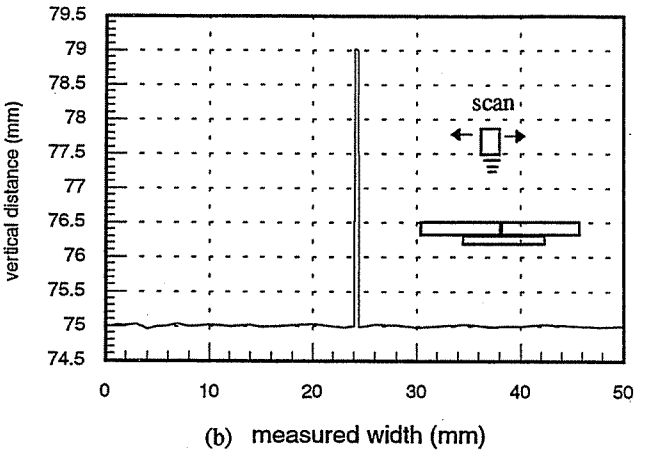

Fig. 10 Measured weld seam profile (a) butt weld with V-groove (b) butt weld without groove

Table 2 Welding parameters and tracking accuracy in GTAW process

Current (A)	Voltage (V)	Speed (m/min)	Standoff (mm)	Shielding gas (SFCH)	Tracking accuracy (mm)	
80	18	0.2	3	18	0.3 H*	0.2 L*
68	15	0.12	2.4	15	0.3 H	0.2L

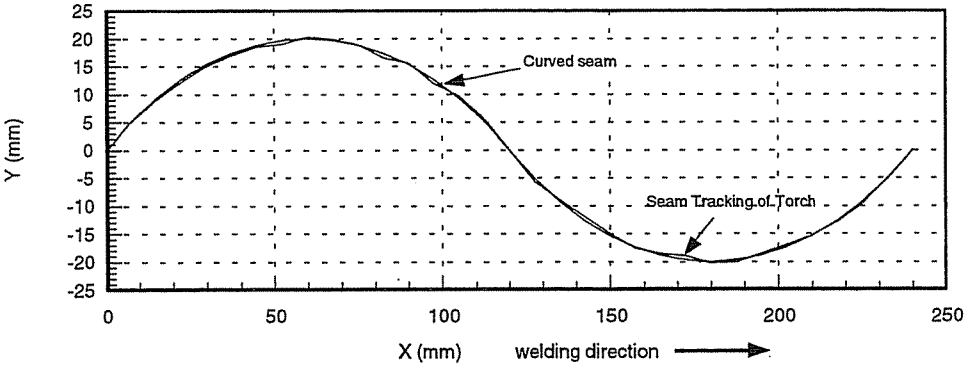

Fig. 11 Seam tracking used in GTAW process

so that the sensor can achieve an optimal resonance frequency and improve the sensitivity of the sensor. In order to match the circuit, the HP-LFA4192 impedance analysis instrument was used to measure the parameters of the equivalent circuit. Table 1 gives the measurements. Based on the measurements and the series resonance principle, the circuit impedance match is done for the sensor. A matching circuit diagram with component values is shown in Fig. 4(*b*). Figure 5(*a*) and (*b*) show the pulse responses of the sensor under its resonance frequency 1.15 MHZ with circuit impedance match and without circuit impedance match. It can be seen that the circuit impedance match has improved the sensitivity of the noncontact ultrasonic sensor.

4 Focus of Acoustic Beam

The transverse resolution of a non-contact ultrasonic sensor depends on the acoustic beam. The diameter of the acoustic beam is smallest at the interface of a near-far acoustic field [13]. Its radius is:

$$r_{-6dB} = 0.35R_s \tag{14}$$

where R_s is the radius of the piezoelectric ceramic. However, the distance from the sensor to the interface of the near-far acoustic field is:

$$Y_0 = R_s^2/\lambda_o \tag{15}$$

where λ_o is the wavelength of the ultrasound in the transducer. When $f_0 = 1$ MHz and $R_s = 13$ mm, $Y_0 = 497$ mm. This figure is much higher than the desired sensor-to-workpiece distance. Also, even in a near acoustic field, the sonic beam is still too wide to be used to accurately identify the seam.

To improve the transverse resolution, a focused transducer needs to be designed to focus the acoustic beam. Figure 6 shows the configuration of the focused ultrasonic sensor. The focused-type transducer utilizes a concave piezoelectric-ceramic PZT-5A and two matching layers of composite of silicon rubber. The radius of the beam at the focal point is:

$$r_{-6dB} = 0.355\lambda_o F/R_s \tag{16}$$

where F is the focal length of the acoustic beam. The depth of focus (Fig. 6) along the beam axis is:

$$L_f = \frac{2G}{G^2 - 1}R \tag{17}$$

where $G = R_s^2/\lambda F$, and R is the radius of a spherical piezoelectric ceramic.

Experiments have been conducted to detect the cross and axial distribution of acoustic pressure for the noncontact ultrasonic sensor with three different focus lengths (Fig. 7). It is found that when $f_0 = 1.5$ MHz, the focal length is small. Because of such a small distance, the sensor may be subjected to possible collision with the workpiece. Also, although the beam can be well focused, the diameter of the beam is very sensitive to the distance between the sensor and the target if the target is off focus. When $f_0 = 0.4$ MHz, the ultrasonic sensor has a longer focus. However, the sonic beam is wider and thus has a lower resolution. When $f_0 = 1.15$ MHz, the ultrasonic sensor produces a sonic beam with a small diameter. This implies a potentially high tracking accuracy. Also, the depth of focus is long enough for sensing the variation in the distance between the sensor and workpiece. In addition, the focal length is about 75 mm so the sensor is not likely to be subjected to any collision with the workpiece. Hence, for seam tracking application, a sensor frequency of about 1.15 MHz is acceptable. Based on available piezoelectric ceramic materials, a noncontact ultrasonic sensor with $f_0 = 1.15$ MHz and 75 mm focus was made to develop the tracking system.

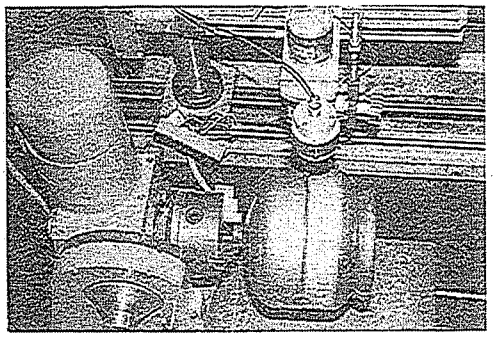

Fig. 12 Welding set-up for tracking round butt weld seam of liquidated gas jars

Table 3 Welding parameters and tracking accuracy in CO_2 welding process

Current (A)	Speed (m/min)	Arc voltage (V)	Shielding gas (SFCH)	Tracking accuracy (mm)
210	0.20	22	15	0.5 H 0.4 L
190	0.17	21	14	0.5 H 0.3 L

The focused noncontact ultrasonic sensors with different frequencies are shown in Fig. 8.

5 Tracking System

The tracking system consists of a noncontact ultrasonic sensor, a scan unit, a signal processor, and a control unit (Fig. 9). The ultrasonic sensor is placed a small distance, L, ahead of the torch (Fig. 9). The sensor is driven by a stepper motor to transversely scan the seam.

During scanning, the distance between the sensor and the scanned point on the workpiece is determined by the timing of the echo. Based on the distance measurements in a scan, the profile of the workpiece along the scanning direction can be obtained to analyze the joint and control the arc length.

Denote r as the scan resolution, i.e., the number of points scanned in a one millimeter (transverse) span. It can be shown based on Fig. 9 that

$$r = f_e / f_c \Delta\theta L \tag{18}$$

where f_e is the frequency of the emitted ultrasonic events, f_c is the step frequency of the stepper motor, $\Delta\theta$ is the angular increment of the stepper motor, and L is the distance between the centers of the sensor and the motor.

Denote the width of the groove as W. It is apparent that

$$W = (P_s - P_L - P_R)/r \tag{19}$$

where P_s is the number of points in a scan, and P_L and P_R are the numbers of points detected on the left and right of the groove, respectively.

The seam deviation with respect to the torch is:

$$\Delta x = (P_L - P_R)/r \tag{20}$$

The resolution of the deviation detection is $1/r$.

Using the scan-mode tracking system, seams with a groove or without a groove can both be recognized and detected. Also, the tracking accuracy is not influenced by the thermal distortion and therefore it can be used in arc welding processes. Figure $10(a)$ shows the measured results in tracking a butt joint with a V-groove. The two crests, the width, and the joint center are obtained. In Fig. $10(b)$, the measured results during tracking a butt joint with a 0.4 mm gap without a groove is illustrated. It can be seen that despite the small gap, the system successfully detected the seam. The resolution and accuracy of the noncontact ultrasonic tracking system is sufficiently demonstrated.

6 Tracking Experiments

Seam tracking experiments have been done for gas tungsten arc welding (GTAW) and CO_2 shielded gas metal arc welding.

6.1 GTAW Seam Tracking. Straight Seam Tracking: In this experiment, the weld seam is straight. The travel direction of the torch deviates 4 deg from the straight seam of a butt joint without a groove. A 4 mm thick mild steel plate with a joint gap of 0.4 mm is used. Welding parameters and tracking accuracy are shown in Table 2. It can be seen that the tracking accuracy is quite satisfactory.

Curvy Seam Tracking: Fig. 11 shows experimental results in tracking a curvy weld seam during a GTAW process. It is apparent that despite the curvature of the weld seam, satisfactory tracking has been achieved.

Application to Steel Jar Welding: Fig. 12 shows the application of the developed tracking system in the welding of liquidated gas steel jars. In this case, the diameter of the steel jar is 200 mm. The width and depth of the groove are 5 mm and 3 mm, respectively. The steel jars are made by punching a 2.5 mm thick steel plate. The manufacturing accuracy of parts to be welded varies from jar to jar. Also, a round butt weld is dealt with. Thus, both the lateral and longitudinal deviations have to be corrected during tracking. By utilizing the developed noncontact ultrasonic sensor, the weld seam has been tracked despite the variation in the parts and round weld path. The tracking accuracy is 0.5 mm in both the lateral and longitudinal directions.

6.2 CO_2 Welding Seam Tracking. Tracking experiments have also been done for CO_2 shielded gas welding. Mild steel plates of 12 mm thickness with a 60° V-groove were used in the experiments. The width of the groove is 11 mm. The torch travels at a direction which deviates 2.6 deg from the seam. Table 3 shows the tracking results and welding parameters. It can be seen that despite the strong spattering and strong arc light associated with CO_2 shielded gas welding, satisfactory lateral and longitudinal tracking accuracies have been obtained.

7 Conclusions

- A noncontact seam tracking system has been developed. Acoustic matching has been performed to increase the transmission efficiencies of high frequency noncontact ultrasonic transducers by 80-fold. Such an increase in the transmission efficiency makes high frequency noncontact ultrasonic sensors useful for seam tracking.
- Because of the use of the high frequency of 1.15 MHz, the diameter of the sonic beam is below 0.5 mm. Hence, this system can actually track nearly any type of weld seam. No grooves or wide gaps are required. Extensive tracking experiments and applications have confirmed the effectiveness of the developed noncontact ultrasonic seam tracking system for arc welding processes.

References

1 Estochen, E. L., and Neuman, C. P., 1984, "Application of Acoustic Sensors to Robotic Seam Tracking," *IEEE Transaction on Industrial Electronics*, Vol. IE-31, No. 3, pp. 219–224.

2 Umeagkwu, C., and Maqueira, B., 1989, "Robotic Acoustic Seam Tracking: System Development and Application," *IEEE Transaction on Industrial Electronics*, Vol. 36, No. 3, pp. 338–348.

3 Cullison, A., and Irving, B., 1992, "Where in the World Is the WELD?" *Welding Journal*, Vol. 71, No. 8, pp. 45–49.

4 Hanright, J., 1986, "Robotic Arc Welding under Adaptive Control—A Survey of Current Technology," *Welding Journal*, Vol. 65, No. 11, pp. 19–24.

5 Agapakis, J. E., and Katz, J. M., 1986, "Joint Tracking and Adaptive Robotic Welding Using Vision Sensing of the Weld Joint Geometry," *Welding Journal*, Vol. 65, No. 11, pp. 33–41.

6 Richardson, R. W., 1986, "Robotic Weld Joint Tracking Systems—Theory and Implementation Methods," *Welding Journal*, Vol. 65, No. 11, pp. 43–51.

7 Zhang, Y. M., Kovacevic, R., and Li, L., 1996, "Adaptive Control of Full Penetration GTA Welding," *IEEE Transactions on Control Systems Technology*, Vol. 4, No. 4, pp. 394–403.

8 Bastos, T. F., 1994, "Weld Seam Detection and Recognition for Robotic Arc-Welding through Ultrasonic Sensors," *IEEE International Symposium on Industrial Electronics,* 94TH0670-0: 310–315.

9 Haller, M. I., and Khuri-Yakub, B. T., 1996, "A Surface Micromachined Electrostatic Ultrasonic Air Transducer," *IEEE Transactions on Ultrasonics Ferroelectrics and Frequency Control,* Vol. 43, No. 1, pp. 1–6.

10 Lach, M., 1991, "An Acoustic Sensor System for Object Recognition," *Sensors and Actuators,* Vol. A26, pp. 541–547.

11 BabicC, M., 1991, "A 20-kHz Ultrasonic Transducer Coupled to the Air with a Radiating Membrane," *IEEE Transactions on Ultrasonics Ferroelectrics and Frequency Control,* Vol. 38, No. 3, pp. 252–255.

12 Munro, W. S. H., and Wykes, C., 1994, "Array for Airborne 100 kHz Ultrasound," *Ultrasonics,* Vol. 32, No. 1, pp. 57–64.

13 Edmods, P. D., 1981, *Ultrasonics,* Vol. 19, Academic Press New York, Landon, Toronto, Sydney, San Francisco.

14 Yano, T., and Tone, M., 1987, "Range Finding and Surface Characterization Using High-Frequency Air Transducers," *IEEE Transactions on Ultrasonics, Ferroelectrics, and Frequency Control,* Vol. UFFC-34, No. 2, pp. 232–236.

15 Mason, W. P., 1972, *Physical Acoustics,* Vol. IX Academic Press New York and Landon.

16 Goll, J. H., 1979, "The Design of Broad-Band Fluid-Loaded Ultrasonic Transducers," *IEEE Transactions on Sonics and Ultrasonics,* Vol. Su-26, No. 6, pp. 385–393.

17 IEEE Standard on Piezoelectricity, 1984, *IEEE Transactions on Sonics and Ultrasonics,* Vol. Su-31, No. 2, pp. 8–55.